Enhanced Aggregation Behavior of Antimony(V) Porphyrins in Polyfluorinated Surfactant/Clay Hybrid Microenvironment

Lucian A. Lucia,[§,†] Tatsuto Yui,[||] Ryo Sasai,[⊥] Shinsuke Takagi,[||] Katsuhiko Takagi,[⊥] Hirohisa Yoshida,[||] David G. Whitten,[§,‡] and Haruo Inoue*[,||,▽]

Department of Chemistry, University of Rochester, Rochester, New York 14627, Department of Applied Chemistry, Graduate Course of Engineering, Tokyo Metropolitan University, 1-1 Minami-ohsawa, Hachiohji-city, Tokyo 192-0397, Japan, Department of Crystalline Materials Science, Graduate School of Engineering, Nagoya University, Furo-cho, Chikusa-ku, 464-8603, Japan, and CREST (Japan Science and Technology), Japan

Received: July 31, 2002

Polyfluorinated surfactant ($C_nF_{2n+1}CONH(CH_2)_2N^+(CH_3)_2C_{16}H_{33}$ Br^-; designated as C*n*F-S, where $n = 1-3$)/clay hybrid compounds have been shown to provide polyfluorinated microcavities in the clay interlayers with molecular dimensions. The aggregation behavior of a water-soluble porphyrin (tetra(4-sulfonatophenyl)-porphyrinatoantimony(V); Sb(V)TSPP) that cointercalates with the surfactant in the polyfluorinated microcavity was investigated. One of the key findings in this study was that the absorption spectra of Sb(V)TSPP molecules that intercalate in the C3F-S polyfluorinated surfactant/clay hybrid microstructures are drastically changed upon dispersion in benzene. The monomer Soret absorption band of Sb(V)TSPP (422 nm) was observed to split into both a longer (438 nm) and a shorter (388 nm) wavelength component. These spectral changes are dependent on the adsorbed amount of Sb(V)TSPP and can be accounted for on the basis of dimer formation. The absorption and emission measurements suggest that two types of dimers (J and H dimers) are formed in the polyfluorinated surfactant/clay hybrid interlayers. It was also found that when the adsorbed amount of surfactant molecules decreased, i.e., when the volume of the polyfluorinated microcavity in the interlayer increased, then the dimerization of Sb(V)TSPP was enhanced. In the case of C2F-S and C1F-S polyfluorinated/clay hybrid compounds, similar spectral behavior arising from dimerization was observed. In contrast, in the case of the hydrocarbon analogues (C3H-S) and cetyltrimethylammonium bromide (CTAB)/clay hybrid compounds, the absorption and emission arising from Sb(V)TSPP indicates that it essentially retains its monomer character. Small-angle X-ray scattering experiments revealed that the clearance space (distance between the layers) for the hybrid compounds in benzene increases compared to that of the solid hybrid compounds. This result indicates a penetration of the benzene molecules into the hybrid layers. It is proposed that the aggregation mechanism of Sb(V)TSPP in polyfluorinated surfactant/clay hybrid compounds obeys the following sequence: (1) formation of a polyfluorinated environment of interlayers that have very weak intermolecular interactions among the surfactant molecules; (2) upon penetration of the benzene solvent molecules, swelling of the hybrid compounds and solvation of Sb(V)TSPP in the interlayers; (3) expulsion of Sb(V)TSPP molecules from the polyfluorinated assemblies into the interlayer space; and (4) migration of Sb(V)TSPP molecules to the microcavities, with concomitant dimer (H and J) formation.

Introduction

Clay minerals possess a layered structure that is characterized by a physical stacking of the alumino-silicate sheets.[1−4] Various ionic molecules can be reversibly inserted into the layered space (viz., by an intercalation process) through general ion-exchange phenomena. This clay layer can self-adjust to accommodate guest species through an increase of the interlayer distances. It is well-known, for example, that intercalated surfactant-type molecules can form molecular assemblies in which the interlayer space allows a regular distribution of guest molecules based on intermolecular interactions.[5−9] Thus, the interlayer space can be "functionalized" or chemically tuned by the judicious choice or inclusion of specific functional compounds. This concept is very interesting and powerful since it can expedite the successful intercalation of a third component into a surface-modified clay layer, providing the possibility of initiating chemical reactions. Intercalation of alkylammonium cation-type surfactants, for example, have been well examined from both applied and basic science perspectives.[10−17]

Polyfluorinated organic compounds are a unique class of organic compounds and have been the subject of recent research activity.[18−22] Their very weak intermolecular interactions with other molecules can be exploited for various applications. For example, an organic fluorinated compound that serves as a solvent is expected to enhance the importance of solute−solute intermolecular interactions, since solvent (fluorinated compound)−solute interactions are known to be minimal in fluorinated

* To whom correspondence should be addressed. E-mail: inoue-haruo@c.metro-u.ac.jp.
† Current address: Institute of Paper Science and Technology, Georgia Institute of Technology, 500 10th Street, N.W. Atlanta, GA 30318-5794.
§ University of Rochester.
|| Tokyo Metropolitan University.
⊥ Nagoya University.
‡ Current address: QTL Biosystems, LLC, 1322 Paseo De Peralta, Santa Fe, NM 87501.
▽ CREST.

10.1021/jp026648a CCC: $25.00
Published on Web 03/28/2003

CHART 1

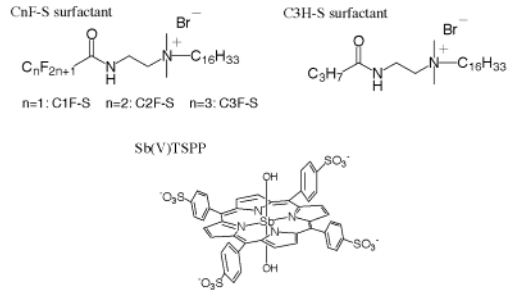

environments.[19,20] Thus, exploration of chemical reactions in polyfluorinated environments is most attractive; yet, there has been little chance to explore perfluorinated compounds as solvents due to their poor miscibility with hydrocarbons. One of the most promising approaches to solve this issue would be the formation of polyfluorinated solvent environments within molecular assemblies such as micelles, reversed micelles, and vesicles. In order to accomplish them, we have synthesized a series of novel ammonium cation-type polyfluorinated surfactants (C*n*F-S, where $n = 1-3$; see Chart 1), which have been found to form micelles and vesicles having unique fluorinated microenvironments at micelle or vesicle/water interfaces.[21,22] We have also found that these polyfluorinated surfactants are easily intercalated into the clay interlayer spaces of sodium saponite (Sumecton SA, used as a cation-exchange-type clay) to form rigidly packed bilayer structures.[23−25] The C3F-S polyfluorinated surfactants exhibit intercalation up to 440% of the cation exchange capacity (CEC) of the saturated adsorption limit of the clay.[23] Remarkably, the clay clearance space (distance between layers) maintains a constant value (ca. 3.0 nm) in the bilayer structures at intercalation levels from 100% to 440% CEC. These results indicate that the polyfluorinated surfactant/clay hybrid compounds have a polyfluorinated microcavity with molecular dimensions that can be easily controlled by the amount of the surfactant intercalation. To clarify the molecular representation of the packing phenomenon, a schematic illustration of the polyfluorinated surfactant (C3F-S)/clay hybrid compounds for various adsorbed amounts of C3F-S is shown in Figure 1.[23]

Two of the most noteworthy aspects of this study are the photophysics and potential photochemistry that are accessible in such polyfluorinated microcavities. The present work describes the application of these cation-exchangeable-type clays for the unique intercalation of metalloporphyrin molecules. We have chosen to study the photophysics and photochemistry of metalloporphyrins since they have been the subject of extensive past research efforts.[26−29] We have therefore initiated a novel investigation of the intercalation behavior of metalloporphyrins in polyfluorinated surfactant/clay hybrid compounds.[25] The tetra(4-sulfonatophenyl)porphyrinatotin(IV) (Sn(IV)TSPP) has been shown to form an aggregate in the interlayers of polyfluorinated surfactant/clay hybrid compounds. The porphyrin aggregates have also received significant attention mainly because of their photochemical and technologically appealing properties.[30−37]

In this investigation, we explored the intercalation and aggregation behavior of tetra(4-sulfonatophenyl)porphyrinatoantimony(V) (Sb(V)TSPP) in sodium saponite clay layers. We also propose an aggregation mechanism for these porphyrins in the polyfluorinated surfactant/clay hybrid environments.

Experimental Section

Materials. The synthesis of polyfluorinated surfactants (C*n*F-S) and their hydrocarbon analogues (C3H-S) has been reported elsewhere.[22] The *n* denotes the number of carbons in the acyl group, F denotes a polyfluorinated surfactant, H denotes a hydrocarbon analogue, and S illustrates a surfactant-type single long alkyl chain. Cetyltrimethylammonium bromide (CTAB; WAKO Pure Chemical Ind. Co.) was recrystallized from acetone.

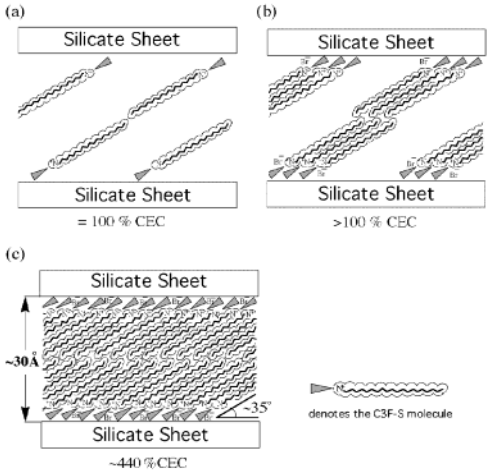

Figure 1. Schematic structure of C3F-S/clay hybrid compounds for various amounts of adsorbed C3F-S molecules: (a) amount approximately equal to CEC, (b) amount in excess of CEC, and (c) 440% CEC. Under the conditions depicted in a or b, the polyfluorinated surfactant/clay hybrid compounds have molecular dimension microcavities in the interlayer. The intercalation levels of surfactant control the size of the microcavity.

The tetra(4-sulfonatophenyl)porphyrinatoantimony(V) (Sb(V)TSPP) was synthesized according to the following procedure: $SbCl_5$ (12 mL) was added dropwise to *meso*-tetra(4-sulfonatophenyl)-21*H*,23*H*-porphyrin dihydrochloride (800 mg, Porphyrin Product, Inc.) in dry pyridine (1 L), and the reaction mixture was stirred for 9 h while refluxing under nitrogen atmosphere to form Sb(V)TSPP. Water (100 mL) was added to the reaction mixture, and the resultant white precipitate was removed by filtration. The filtrate solution was evaporated. The crude Sb(V)TSPP was purified by reprecipitation from acetonitrile, gel filtration, (Sephadex LH-20, eluent; H_2O), and column chromatography (SiO_2, eluent; acetonitrile/H_2O = 4:1). The purple fraction was collected and identified as [Sb(V)TSPP-$(OH)_2$]Cl. Yield: 31%. ^{1}H NMR (δ/ppm) in D_2O: 8.19 (8H, d), 8.40 (8H, d), 9.56 (8H, s). UV−vis (λ/nm, (log ϵ)) in H_2O: 415.0 (5.73), 547.0 (4.29), 586.6 (3.91). The structures of the C*n*F-S and C3H-S surfactants and Sb(V)TSPP are shown in Chart 1.

Cation-exchangeable clays were used in the present work. Sumecton SA (Kunimine Co.) is a type of sodium saponite synthesized via a hydrothermal reaction. It has good transparency in the visible region. The chemical and physical characteristics of Sumecton SA include the following:[38] The composition is $[(Si_{7.20}Al_{0.80})(Mg_{5.97}Al_{0.03})O_{20}(OH)_4]^{-0.77}(Na_{0.49}Mg_{0.14})^{+0.77}$, the surface area is 750 m^2 g^{-1}, and the cation exchange capacity (CEC) is 0.997 meq g^{-1}.

Deionized water (conductivity <0.02 μS cm^{-1}) was used as a solvent for the intercalation reactions. Benzene (Kanto; spectroscopic grade) was used for all spectroscopic studies.

Sample Preparation. The synthesis of surfactant/clay hybrid compounds and cointercalation of Sb(V)TSPP were carried out according to the following procedure:[23−25] In a typical example, 60 mL of aqueous surfactant solution (5 mM) and 4 mL of aqueous Sb(V)TSPP solution (7.9×10^{-5} M) were added to 10 mL of clay dispersion (10 g L^{-1}). Under these conditions,

the loading levels (amounts present in the suspension) of surfactant and Sb(V)TSPP were 300% and 0.16%, respectively, with respect to the CEC of the clay. We were able to control the levels of the adsorbed surfactant and Sb(V)TSPP via control of the corresponding loading levels. An aqueous mixture of Sb(V)TSPP/surfactant/clay was stirred at 60−70 °C for 3 h. The precipitate was filtered (ADVANTEC, Toyo Roshi Kaisha, Ltd.; pore size = 0.2 μm), washed with water on filter paper, and dried in air at 80 °C to constant weight. The relative composition of the clay/surfactant hybrid compounds was determined from the weight gain in the clay and independently confirmed by elemental analysis.[23] The amount of adsorbed Sb(V)TSPP was calculated from the residual amount of Sb(V)TSPP in the filtrate solution.

Instrumentation and Methods. The solid surfactant/clay hybrid compounds were dispersed in benzene for measurements of the absorption and emission spectra of the guest porphyrin molecules. The benzene dispersion of the hybrid compound was carried out by addition of dried solid hybrid compound into benzene stirred at 23 ± 1 °C. For the aggregation experiment, the benzene dispersion was continuously stirred at 23 ± 1 °C, and the absorption spectrum was measured as a function of time. The benzene dispersion formed a precipitate after standing overnight, but when the resulting dispersion was stirred again, stable reproducible spectra were observed.

The polarized dichroic absorption spectra were measured for cast films of surfactant/clay/Sb(V)TSPP hybrid compound. The cast films were prepared by casting a benzene dispersion of hybrid compound onto a quartz glass plate which was air-dried at room temperature. The XRD profiles of surfactant/clay/Sb(V)TSPP cast films from benzene were essentially the same as that for the solid surfactant/clay/Sb(V)TSPP. The parallel orientation of the hybrid layer against the glass plate was confirmed by XRD and SEM.[25]

The absorption spectra were recorded on a UV-2400 (Shimadzu) spectrophotometer. The steady-state emission spectra were obtained on an F-4010 spectrofluorometer (Hitachi). The dichroic absorption spectra were recorded on a V-550 spectrophotometer (JASCO) equipped with a polarizer unit.

A small-angle X-ray scattering (SAXS) instrument was attached to the small-angle X-ray scattering optics (DSC-SRXRD) at beam-line BL-10C at the Photon Factory (PF), High Energy Accelerator Research Organization (KEK), Tsukuba, Japan. The wavelength of the monochromatic X-rays for DSC-SRXRD was 0.1488 nm. The scattered X-rays were detected by a one-dimensional position-sensitive proportional counter (PSPC). The distance between the specimen and the PSPC was 680 mm, so that a range of 1.25 nm < $S^{-1} = ((2/\lambda)\sin\theta)^{-1}$ < 200 nm was covered, where 2θ is the scattering angle and λ is the X-ray wavelength. The sample cell was made from Teflon with a Kapton window for the benzene dispersion. The observed intensities were corrected for transmission and subtracted from the intensity of the blank measurement using an empty cell.

Results and Discussion

Cointercalation of Sb(V)TSPP into the Surfactant/Clay Hybrid Layer. Addition of an aqueous solution of C3F-S surfactant and Sb(V)TSPP to an aqueous clay dispersion results in formation of a brown precipitate. Soret absorption maxima for the mixture are red-shifted 4 nm from that observed for Sb(V)TSPP in aqueous solution, indicating an intercalation of Sb(V)TSPP into the clay layer, as will be described later. On the basis of the described gravimetric quantification procedure (see Experimental Section), it was found that the brown precipitate was a surfactant/clay/Sb(V)TSPP hybrid compound. The amount of surfactant incorporated and the layer distances (d = ~3.0 nm) were unaffected by the cointercalation of Sb(V)TSPP. This result demonstrates that the Sb(V)TSPP molecules do not disturb the structure of the hybrid compound at the very light loading levels used in the present work (0.05−0.2% vs CEC).

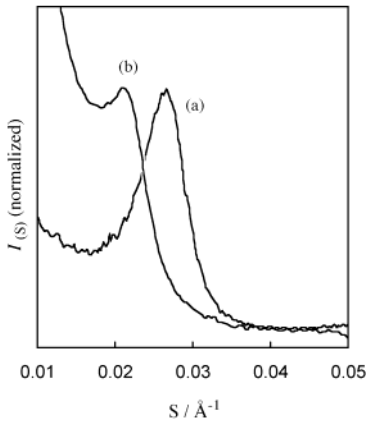

Figure 2. Small-angle X-ray scattering profiles for C3F-S/clay hybrid compounds (C3F-S = 270% CEC): (a) dry film and (b) benzene dispersion.

It should be noted that the anionic Sb(V)TSPP molecule alone was not able to be intercalated into the negatively charged cation-exchange-type clays (Sumecton SA) due to electrostatic repulsion. Sb(V)TSPP could, however, be successfully intercalated in the presence of an ammonium cation-type surfactant by forming an ionic association complex[22,34−36,39] between the ammonium surfactant and Sb(V)TSPP. The anionic Sb(V)TSPP is therefore believed to associate and exist in close proximity to the ammonium headgroup of the surfactants and thus be cointercalated.[24,25,34,40]

Swelling Behavior of Polyfluorinated Surfactant/Clay Hybrid Compounds in Benzene. When the polyfluorinated surfactant/clay hybrid compounds are dispersed in benzene, the resultant solution is transparent in the visible region. The spectral transparency is likely a result of the coincident refractive indices between benzene and the clay that has swollen with the solvent. When the benzene dispersions of the hybrid compounds containing Sb(V)TSPP were filtered through a membrane filter made of Teflon (0.2 μm), it was found that there was no measurable absorption from Sb(V)TSPP in the filtrate solution. This result indicates that the Sb(V)TSPP molecules were incorporated into the hybrid compound, even when dispersed in benzene. The fairly good dispersion of the intercalated hybrid compound in benzene suggests good swelling in the solvent.[24,25]

To more fully describe the nature of the structure of the hybrid compound in the benzene dispersion, small-angle X-ray scattering (SAXS) measurements were carried out. One of the principal questions that was addressed was whether the hybrid compounds maintained their lamellar structure or not when dispersed in benzene. The SAXS profiles of the C3F-S/clay hybrid compound benzene dispersion and solid film are shown in Figure 2. The sharp d(001) diffraction peak due to the layered structure was observed for both the solid film and the benzene dispersion. This suggests that the C3F-S/clay hybrid compound maintained a layered structure even when dispersed in benzene. The estimated clearance space (distance between the layers) was 3.0 nm for the solid film and 3.8 nm for the benzene dispersion. This expansion of the clearance space clearly demonstrates the penetration of the benzene molecules into the clay layer.

It is therefore proposed, on the basis of the SAXS and spectral absorption data, that the bilayer structure is maintained by the incorporation of benzene molecules between each surfactant layer, in a sandwich-type structure.

Aggregation Behavior of Sb(V)TSPP in Polyfluorinated Surfactant/Clay Hybrid Layer Swollen with Benzene. The aqueous mixture of C3F-S/clay/Sb(V)TSPP hybrid compound has a signature Soret maximum that could readily be assigned to the monomer of Sb(V)TSPP (419 nm), but it was slightly red-shifted from that observed in aqueous solution (415 nm). To further explore the behavior of the porphyrins as a function of environment, a solid film of the aqueous mixture of C3F-S/clay/Sb(V)TSPP was obtained by filtering and drying the C3F-S/clay/Sb(V)TSPP aqueous solution (see Experimental Section). The solid film exhibited a more red-shifted Soret absorption maximum (422 nm). It is known that the Soret absorption maxima of metalloporphyrins are sensitive to solvent polarity: in a less polar environment, the absorption maxima are shifted toward the red.[41] The observed red-shift of the Soret band can be explained by a decrease in the polarity of the microenvironment surrounding the intercalated Sb(V)TSPP guest molecules (419 nm)[22,24,25] and the severe attenuation of polarity due to the vaporization of water in the drying process (422 nm). The aqueous mixture and solid film had Soret maxima that were characteristic of the nonaggregated Sb(V)TSPP, indicating that the Sb(V)TSPP molecules exist as a monomer within the interlayer space, even during the mixing with the surfactant/clay, the solid film formation, and the drying procedures.

Yet, upon dispersion of the dry solid film of C3F-S/Sb(V)-TSPP/clay (C3F-S/Sb(V)TSPP = 270:0.12% vs CEC) in benzene, the Soret band of Sb(V)TSPP drastically changed (Figure 3a). During the first 60 min of dispersion, the Soret band exhibited a monomer-like absorbance at 422 nm. During the subsequent 1.5 h, the 422 nm monomer band diminished, and new 388 and 438 nm bands were observed with two clean isosbestic points at 393 and 431 nm. This spectral change achieved a steady-state distribution after approximately 25 h. Excitation of the initial 422 nm band provided the monomer fluorescence spectrum at 597 and 652 nm, whereas excitation of the 438 nm envelope gave 602 and 659 nm emission bands, with much lower emission intensities than observed for the monomer. Furthermore, excitation of the 388 nm band gave almost no emission intensity. These results strongly suggest that the 388 and 438 nm absorption bands are associated with different species. The emission quantum yield of porphyrins is recognized to diminish through aggregate formation. These results are consistent with an aggregation phenomenon of the Sb(V)TSPP guest molecules within the interlayer space of the surfactant/clay hybrid compounds. A J-type porphyrin dimer is known to have a red-shifted λ_{max} and a weak fluorescence, while an H-type one exhibits a blue-shift of the absorption and is almost nonemissive.[37] The blue-shifted 388 nm and the red-shifted 438 nm species, thus, can be accurately described as dimers of the H-type and J-type, respectively.[25−27,30−37,42,43] Penetration of benzene molecules into the interlayer is suggested to be a critical step in the formation of the Sb(V)TSPP aggregates. The spectral change with the two isosbestic points strongly suggests that the H-type and J-type dimers are formed from monomer in a constant ratio, as described later.

The same experiments were carried out for the C2F-S and C1F-S polyfluorinated surfactant/Sb(V)TSPP/clay hybrid compounds (C2F-S/Sb(V)TSPP = 160:0.12, C1F-S/Sb(V)TSPP = 170:0.12% vs CEC, respectively), and similar absorption spectral changes were observed (Figure 3b,c). Very interestingly, the monomer Sb(V)TSPP absorption remained unchanged after 100 hours of benzene dispersion in the surfactant/clay hybrid compounds containing the hydrocarbon-type surfactant C3H-S and CTAB hybrid compounds (C3H-S/Sb(V)TSPP = 170:0.12, CTAB/Sb(V)TSPP = 170:0.12% vs CEC, respectively). The latter result clearly indicates that the H- and J-dimerization phenomenon is only enhanced in the polyfluorinated environment. The strong lipophobic character of the perfluorinated alkyl chain may expel the surrounding hydrophobic Sb(V)TSPP molecules, to promote the aggregation. The benzene solvent would then assist in their migration within the interlayer of the hybrid compound through the swelling process.

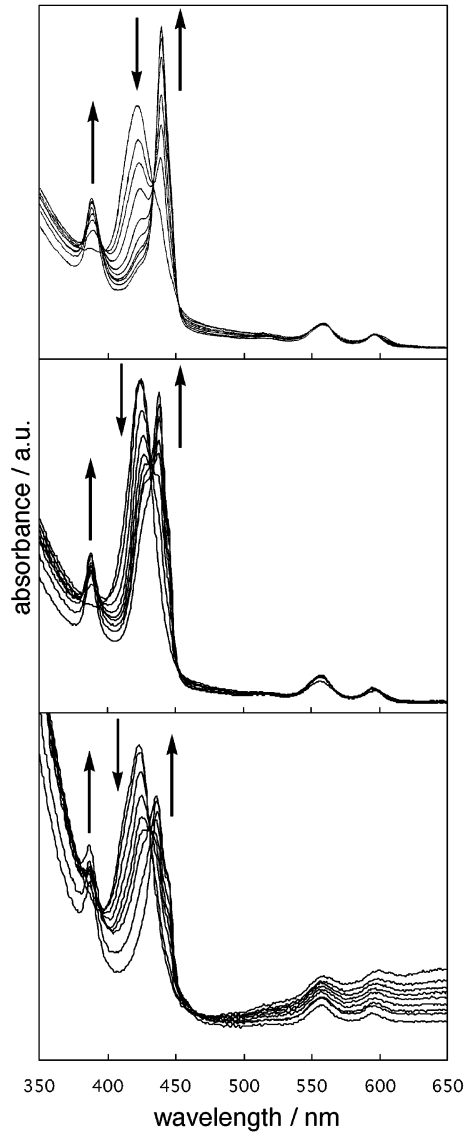

Figure 3. Absorption spectral changes of Sb(V)TSPP cointercalated in the polyfluorinated surfactant/clay hybrid compounds upon benzene dispersion: (a) C3F-S/Sb(V)TSPP = 270:0.12% CEC, (b) C2F-S/Sb-(V)TSPP = 160:0.12% CEC, and (c) C1F-S/Sb(V)TSPP = 170:0.12% CEC hybrid compounds.

Effect of Adsorbed Amount of Sb(V)TSPP on Aggregation. To more closely examine the aggregation behavior of Sb-(V)TSPP, the influence of the amount of adsorbed Sb(V)TSPP was examined for C3F-S/Sb(V)TSPP = 270:0.12−0.04% vs CEC hybrid compounds.[25] The differences in absorption, $\Delta\Delta OD_t$, at two fixed wavelengths $\lambda_1 = 422$ nm (monomer band) and $\lambda_2 = 438$ nm (J-dimer band), defined in eq 1 were plotted against time, as shown in Figure 4a. The plots for H-dimer

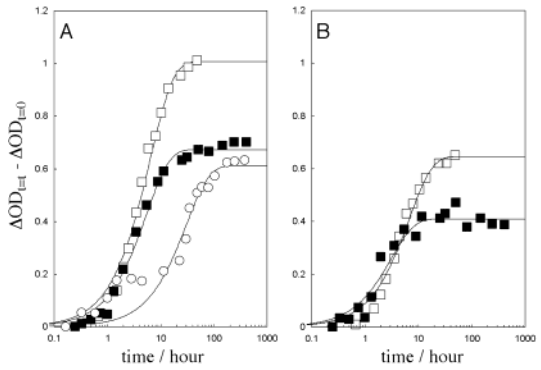

Figure 4. Effect of the amount of adsorbed Sb(V)TSPP on the spectral changes in C3F-S (270% CEC)/clay hybrid compounds: (A) analyzed at $\lambda_1 = 422$ nm, $\lambda_2 = 438$ nm (J-dimer formation), and (B) analyzed at $\lambda_1 = 422$ nm, $\lambda_2 = 388$ nm (H-dimer formation). Adsorbed amounts of Sb(V)TSPP were 0.12% (□), 0.08% (■), 0.06% (○) CEC.

formation, where $\lambda_1 = 422$ nm (monomer band) and $\lambda_2 = 388$ nm (H-dimer band), were also shown in Figure 4b, where $(OD_{\lambda i})_0$ and $(OD_{\lambda i})_t$ denote the observed absorbances for wavelength λ_i at $t = 0$ and t, respectively. The $\Delta\Delta OD_t$ term effectively removes the scattering effect of incident light by the subtraction procedure in eq 1. As shown in Figure 4, within the initial hour, the Sb(V)TSPP molecules retained their monomer-type absorption character for all adsorbed amounts of Sb(V)TSPP upon dispersion in benzene. The absorption spectral changes commenced after approximately 1.5 h and stabilized after approximately 25 h in the benzene dispersion. These results indicate that the time required for penetration of the benzene molecules and subsequent migration of the porphyrins under the conditions is roughly 1.5 h.

$$\Delta\Delta OD_t = (OD_{\lambda 2} - OD_{\lambda 1})_{t=0} - (OD_{\lambda 2} - OD_{\lambda 1})_{t=t} \quad (1)$$

The Sb(V)TSPP aggregate formation was enhanced by increasing the adsorbed amount of Sb(V)TSPP. On the other hand, the absorption spectra (not shown) were essentially unchanged even upon prolonged standing of the benzene dispersion for the two samples in which the adsorbed amount of Sb(V)TSPP was 0.04% and 0.05% CEC, indicating that no aggregate formation occurred. This suggests that the critical adsorbed amount of Sb(V)TSPP to facilitate aggregate formation is approximately 0.05% CEC. Since Sumection SA clay has an area of 1.25 nm^2 per anion site,[44] when the adsorbed amount of Sb(V)TSPP was 0.05% versus CEC, the surface area divided by the number of Sb(V)TSPP molecules (area occupied by one Sb(V)TSPP molecule) is estimated to be 2500 nm^2 (=1.25 nm^2/0.0005). This result implies that the area covered in the random movement of the Sb(V)TSPP molecules is approximately 2500 nm^2 (=50 nm × 50 nm), suggesting that the effective average area for the interlayer spaces in the hybrid compound is 2500 nm^2. This estimate coincides well with the primary particle size characteristic of Sumecton SA (several tens of nm), as determined by dynamic light scattering method.

Assuming J-dimer (D_J), H-dimer (D_H) formation, and the equilibrium between them as described in eqs 2−4), the kinetics of the two types of dimer formation are expressed by eqs 5−6:

$$M + M \underset{k_{-1J}}{\overset{k_{1J}}{\rightleftharpoons}} J{-}D \quad (2)$$

$$M + M \underset{k_{-1H}}{\overset{k_{1H}}{\rightleftharpoons}} H{-}D \quad (3)$$

$$J{-}D \underset{k_{-2}}{\overset{k_2}{\rightleftharpoons}} H{-}D \quad (4)$$

$$\frac{d[J{-}D]}{dt} = k_{1J}[M]^2 + k_{-2}[H{-}D] - (k_{-1J} + k_2)[J{-}D] \quad (5)$$

$$\frac{d[H{-}D]}{dt} = k_{1H}[M]^2 + k_2[J{-}D] - (k_{-1H} + k_{-2})[H{-}D] \quad (6)$$

$$\frac{[H{-}D]}{[J{-}D]} = \beta \quad [J{-}D] = C_0 X \quad [H{-}D] = C_0 \beta X \quad (7)$$

, where k_{1J}, k_{-1J}, k_{1H}, and k_{-1H} are the rate constants of formation and dissociation of the J-type dimer and H-type dimer porphyrin, respectively. The k_2 and k_{-2} are rate constants for the equilibrium between the J-type and H-type dimers. J−D, H−D, and M denote the J-type dimer, H-type dimer, and monomer. As shown in Figure 3, the absorption spectra corresponding to the monomer and J- and H-dimers have clear isosbestic points. This indicates that the formation ratio of J- and H-dimers is constant, as expressed by eq 7, where C_0, X, and β represent the initial concentration of monomer Sb(V)TSPP, molar fraction of J-type dimer, and the ratio between H- and J-dimer. The molar fraction X at time $= t$ can be expressed by eq 8, from the relationships among eqs 5−7.

$$X = E\left(\frac{1 - e^{-Gt}}{1 - Fe^{-Gt}}\right) \quad (8)$$

where

$$E = \frac{B - \sqrt{B^2 - 4AC}}{2A}$$

$$F = \frac{B - \sqrt{B^2 - 4AC}}{B + \sqrt{B^2 - 4AC}}$$

$$G = \sqrt{B^2 - 4AC}$$

$$A = 4C_0 k_{1J}(1 + \beta)^2$$

$$B = 4C_0 k_{1J}(1 + \beta) + k_{-1J} + k_2 - \beta k_{-2}$$

$$C = 4C_0 k_{1J}$$

The $\Delta\Delta OD_t$ term in eq 1 can be further expressed as eq 9, assuming dimer formation:

$$\Delta\Delta OD_t = C_0[(\epsilon_M^{\lambda 1} - \epsilon_M^{\lambda 2})(1 + \beta) + (\epsilon_J^{\lambda 1} - \epsilon_J^{\lambda 2}) + (\epsilon_H^{\lambda 1} - \epsilon_H^{\lambda 2})\beta]X$$
$$= C_0[(\Delta\epsilon_M(1 + \beta) + \Delta\epsilon_J + (\Delta\epsilon_H)\beta]X \quad (9)$$

where $\Delta\epsilon_M$, $\Delta\epsilon_J$, and $\Delta\epsilon_H$ denote differences in the absorption coefficients of the monomer, J-dimer, and H-dimer at λ_1 (=422 nm) and λ_2 (=438 or 388 nm). Equation 9 can be rewritten as eq 10. Using the relationships in eq 10, curve-fitting for the plots in Figure 4 was carried out by varying the three parameters F, G, and H. The curves fit very well to the experimental data, as shown in Figure 4.

$$\Delta\Delta OD_t = H\left(\frac{1 - e^{-Gt}}{1 - Fe^{-Gt}}\right) \quad (10)$$

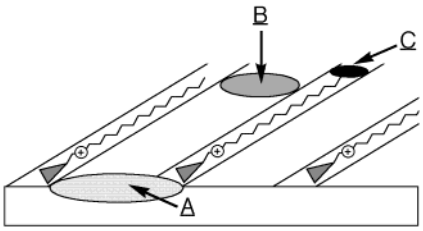

Figure 5. Schematic drawing of proposed surfactant/clay hybrid microstructure and relationships between the definitions of the following three areas: (A) occupied area; (B) excess area; and (C) cross-sectional area of alkyl chains (26 Å^2).

where

$$H = C_0[(\Delta\epsilon_M(1+\beta) + \Delta\epsilon_J + (\Delta\epsilon_H)\beta)E$$

Very interestingly, each curve for J-dimer (λ_{max} = 438 nm) and H-dimer (λ_{max} = 388 nm) formation at the Sb(V)TSPP concentration of 0.12% versus CEC gave almost the same values for parameters F and G: For J-dimer formation, $F = 1.01 \times 10^{-13}$ and $G = 0.157$ s^{-1}, and for H-dimer formation, $F = 1.01 \times 10^{-13}$ and $G = 0.149$ s^{-1}, respectively. The good coincidence of the parameters for J- and H-dimer formation strongly supports the idea that J-dimer and H-dimer are formed in a constant ratio from the monomer porphyrin. Each rate constant (k_{1J}, k_{-1J}, k_{1H}, k_{-1H}, k_2, and k_{-2}), the ratio β, $\Delta\epsilon_J$, and $\Delta\epsilon_H$, however, could not be determined here owing to the limited number of parameters obtained from the simulation.

Surfactant Concentration Effect. The adsorbed amount of polyfluorinated surfactant can be controlled without changing the clay interlayer distance to maintain a constant value (in the case of C3F-S polyfluorinated surfactant, the intercalated levels are 100−440% vs CEC). This suggests that the polyfluorinated surfactant/clay hybrid compounds have given rise to size-variable polyfluorinated microcavities.[23] It was expected that, on the basis of the adsorbed amount of surfactants, or more appropriately, the volume of the microcavity (excess area) in the interlayer, the aggregation of Sb(V)TSPP would be affected. The characteristics of the microcavities can be expressed in terms of the "occupied areas" and "excess areas", as shown in Figure 5. The "occupied area" (area *A* in Figure 5) is defined as the value of the surface area of the clay (125 Å^2/anionic site)[44] divided by the value of mole fraction of the adsorbed amount of surfactant versus CEC.[23] The "excess area" (area *B* in Figure 5) is defined as the value obtained by subtraction of the cross-sectional area of the most rigidly packed alkyl chain of an ammonium-type surfactant (26 Å^2: area *C* in Figure 5)[23,45−47] from the observed occupied area of each surfactant. Aggregation experiments were therefore carried out to test the effect of the size of the microcavity by employing various adsorbed amounts of surfactant, while the adsorbed amount of Sb(V)TSPP was fixed at 0.12% CEC. The adsorbed amounts of surfactant, the occupied areas of each surfactant molecule, and the excess areas in the interlayer are listed in Table 1.

In the case of the C2F-S and C3F-S/clay hybrid compounds, clear relationships between the adsorbed amounts of polyfluorinated surfactants and aggregation behavior were observed. Control of the adsorbed amounts of surfactant was difficult for C1F-S, C3H-S, and CTAB, mainly because of their saturated adsorption limits (approximately 200% CEC).[23] As described previously, Sb(V)TSPP dimers appear following about 1.5 h of benzene dispersion, and they stabilized after 25 h in the hybrid compound containing C3F-S = 270% CEC. In the case of the hybrid compound containing C3F-S = 170% CEC, very fast aggregate formation was observed. The Sb(V)TSPP aggregate appeared within 10 min of dispersion in benzene and stabilized after 6 h. For the hybrid compound containing C3F-S = 330% CEC, the monomer Sb(V)TSPP nature remained unchanged even after prolonged standing, in excess of 60 h. A similar phenomenon was observed for C2F-S/clay hybrid compounds. The Sb(V)TSPP aggregated in the hybrid compound containing C2F-S = 160% CEC within 10 h. In contrast, the monomer Sb(V)TSPP remained unchanged even after prolonged standing (in excess of 60 h) in the hybrid compound containing C2F-S = 250% CEC. The Sb(V)TSPP formed an aggregate in the hybrid compounds containing C1F-S = 170% CEC within 25 h. Again, the monomer Sb(V)TSPP remained unchanged even after prolonged standing (in excess of 60 h) in the hybrid compound containing hydrocarbon-type surfactants (C3H-S, CTAB = 170% CEC).

TABLE 1: Relation between the Adsorbed Amount of Surfactant and Aggregate Formation of Sb(V)TSPP[a] in the Interlayer Space

surfactant	adsorbed amount of surfactant, % CEC	occupied area, Å^2	excess area, Å^2	aggregate formation
C3F-S	330	38	12	no
	270	46	20	yes
	170	74	48	yes (very fast)
C2F-S	250	50	24	no
	160	78	52	yes
C1F-S	170	74	48	yes
C3H-S	170	74	48	no
CTAB	170	74	48	no

[a] Adsorbed amount of Sb(V)TSPP is 0.12% CEC.

Remarkably, Sb(V)TSPP remained as a monomer in the hydrocarbon-type surfactant (C3H-S and CTAB) hybrid compounds, even though they have the same excess area as that found for C1F-S. These results confirm that the polyfluorinated microenvironment in the interlayer space of the clays is critical to enhancing the aggregation of Sb(V)TSPP, mainly due to the expelling of Sb(V)TSPP by the polyfluorinated alkyl group of the surfactant.

Influence of Microscopic Orientation of Sb(V)TSPP in Polyfluorinated Surfactant/Clay Hybrid Compounds on Aggregation. Part of this work attempted to more clearly define how certain microcavity constraints affected the guest packing, specifically, with respect to the tilt angle of the porphyrin plane. One of the primary issues of interest in this regard was determining how the metalloporphyrins orient themselves in the interlayer of the clay with respect to the polyfluorinated surfactants. Polarized dichroic absorption measurements[25,48−51] were carried out for the determination of the molecular tilt angle of Sb(V)TSPP in the hybrid compound. Both the nonaggregated state and aggregated forms of Sb(V)TSPP in the hybrid compound from benzene dispersion were cast on quartz glass plates (see Experimental Section).

The relation between the rotation angle (α) of the substrate (or incident angle) and dichroic ratio (R) for uniaxial orientation is expressed as eq 11:[52,53]

$$R = A_y/A_x = \{2[\sin^2\theta + \sin^2\alpha(3\cos^2\theta - 1)] - (3\cos^2\theta - 1)(3\cos^2\theta - 1)\sin^2\gamma\}/\{2\sin^2\theta + (2 - 3\sin^2\theta)\sin^2\gamma\} \quad (11)$$

where A_y, A_x, θ, and γ represent the absorption intensities for the vertical and horizontal polarized incident light, the angle of the molecular axis relative to the optical transition moment, and

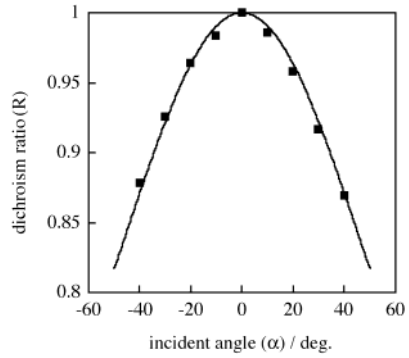

Figure 6. Experimental relationship between the dichroism ratio (*R*) and the angle of incidence (α) of the C3F-S/Sb(V)TSPP = 270:0.12%/ clay hybrid cast film at the Soret monomer absorption band (422 nm); the solid line was calculated from eq 11.

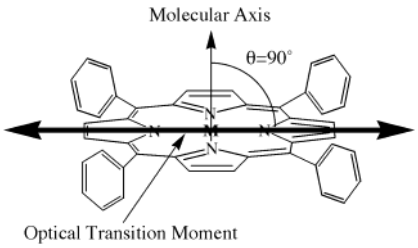

Figure 7. Schematic diagram of the orientation of the electronic transition moment and the molecular axis of the porphyrin molecule. The Soret absorption is caused by this transition moment. The transition moment exists in the plane of the porphyrin ring.

TABLE 2: Tilt Angles of MTSPPs in C3F-S/Clay Hybrid Microstructures

MTSPP	state	γ (deg)
Sb(V)TSPP	monomer	45.7
	H-dimer	47.0
	J-dimer	44.9
Sn(IV)TSPP[a]	monomer	11.7
Ge(IV)TSPP[a]	monomer	30.3

[a] Reported values in ref 25.

the tilt angle of the molecule to the substrate normal, respectively. Figure 6 shows the experimental correlation between the α-angle and the dichroic ratio (*R*) of the monomer Sb(V)TSPP in the interlayer space of a C3F-S/clay hybrid cast film (C3F-S/Sb(V)TSPP = 270:0.12% CEC) measured at the Soret monomer absorption maxima (422 nm).

The *R* value depends on the α-angle and exhibited a maximum at α = 0°. This indicates that the Sb(V)TSPP molecules are oriented not only in the clay but also subsequently on the glass plate, since the hybrid clay particles are aligned in the film. The Soret absorption of Sb(V)TSPP arises from the π-electron conjugation in the porphyrin plane; thus, the optical transition moment of Soret absorption exists in the plane of the porphyrin ring. The molecular axis of Sb(V)TSPP is defined as a normal line in the porphyrin plane, and the angle (θ) of the molecular axis to the optical transition moment is estimated to be 90° (Figure 7). By fitting eq 11 to the correlation between *R*, α, and θ, the tilt angle (γ) of Sb(V)TSPP was estimated. The solid line in Figure 6 is the fitting result based on eq 11. It can be seen that the experimental data was well fitted by eq 11, and the estimated tilt angles of Sb(V)TSPP in various states are listed in Table 2. The monomer Sb(V)TSPP orients itself 45.7° relative to the clay layer. Similar experiments were carried out for the H-dimer (analyzed at 388 nm) and the J-dimer (analyzed at 438 nm) of Sb(V)TSPP in the C3F-S/clay hybrid

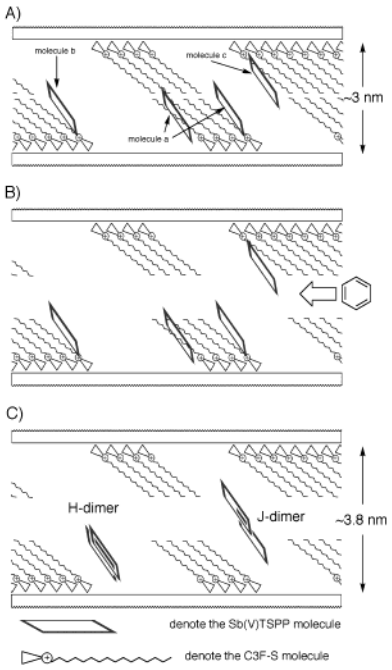

Figure 8. Schematic depiction of the aggregation mechanisms of Sb(V)TSPP in polyfluorinated surfactant/clay hybrid compounds: (A) solid state; (B) swollen in benzene (the clay layer expands due to incorporation of benzene molecules); and (C) migration of Sb(V)TSPP molecules into the interlayer, with subsequent dimer formation.

compounds. The dipole moments of the H- and J- dimers are tilted 47.0° and 44.9° versus the clay layer, respectively.

On the basis of the X-ray analysis, the C3F-S molecules might orient themselves approximately 35° relative to the clay layer.[23] The tilt angles for Sb(V)TSPP are different from that of the C3F-S polyfluorinated surfactant, showing that the orientations of the Sb(V)TSPP molecules are independent of the orientation of the C3F-S molecules. It is thought that the Sb(V)TSPP molecules are located outside of the oriented C3F-S polyfluorinated surfactant assemblies and are weakly associated with the ammonium cation of C3F-S. The benzene solvent, thus, could easily transport Sb(V)TSPP molecules for aggregation.

The Sb(V)TSPP molecules can orient themselves in nonparallel orientations versus the clay surface and may thus be able to induce the formation of the two types of dimers (H and J), as described previously, in which the clearance space of the hybrid compounds is estimated to be about 30 Å.[23] Yet, this clearance distance can sufficiently accommodate the Sb(V)TSPP molecule (diagonal direction of SO_3^- to SO_3^- of Sb(V)TSPP is ca. 20 Å). This might mean that the degrees of translational freedom of Sb(V)TSPP in the direction normal to the clay layer are relatively high. Thus, the two types of dimers can be formed simultaneously. One includes a stacked orientation of the two porphyrin rings (strongly π-conjugated H-dimer), while the other is described as two porphyrin rings oriented in a staggered structure (weakly π-conjugated J-dimer). Supposing a Poisson distribution of Sb(V)TSPP in the interlayer of the clay, the two porphyrins situated on the same surface of the clay (molecules a and b in Figure 8) may form an H-type dimer, while they form a J-type dimer when the two molecules are adsorbed on opposite surfaces of the clay layer within the same interlayer (molecules a and c in Figure 8). In this case, the tilt angle of the porphyrin plane versus the clay layer would not be altered much upon J- and H-dimer formation. The proposed dimerization mechanisms of Sb(V)TSPP in the polyfluorinated surfactant/clay interlayer are shown in Figure 8.

In contrast, it was found that Ge(IV)TSPP molecules orient themselves 30.3° with respect to the clay surface, with no concomitant dimer formation for Ge(IV)TSPP having a similar C3F-S tilt angle; apparently, the Ge(IV)TSPP is deeply trapped within the surfactant assemblies in the interlayer of the clay. The Sn(IV)TSPP molecules orient themselves 11.7° with respect to the clay surface (almost parallel to the clay surface), but selective H-dimer formation for Sn(IV)TSPP was observed.[25] The two Sn(IV)TSPP molecules adsorbed on the two opposing surfaces of the clay may not be able to form a J-type dimer owing to the overly long distance between the two porphyrin planes, which are almost parallel to the clay surface.

Conclusions

The spontaneous aggregation phenomenon of Sb(V)TSPP molecules that are intercalated in polyfluorinated surfactant/clay hybrid compounds was investigated. The aggregation behavior was observed only with polyfluorinated-type surfactants. Two types of dimers (H- and J-dimers) were observed simultaneously. A clear enhancement of aggregation was observed by increasing the adsorbed amount of Sb(V)TSPP, and a curve-fitting that assumed dimer formation provided a good fit to the experimental results. The aggregation was inhibited by increasing the adsorbed amount of surfactant or by decreasing the excess area (polyfluorinated microcavity). Dichroic absorption spectra measurements revealed that the Sb(V)TSPP molecules in the interlayer of the C3F-S/clay hybrid compound orient themselves at an angle of 45.7° with respect to the clay layer.

On the basis of these results, it is proposed that the aggregation mechanism of Sb(V)TSPP in the polyfluorinated surfactant/clay interlayer is as follows: (1) Sb(V)TSPP in the surfactant/clay hybrid exists in a nonaggregated state, prior to benzene dispersion (Figure 8a). (2) With penetration of benzene molecules, there is swelling and an increase in fluidity of the interlayer (Figure 8b). (3) There is rejection of Sb(V)TSPP from the polyfluorinated environment and random movement in the excess space in the hybrid layer, in which the area available for movement of Sb(V)TSPP is estimated to be ca. 2500 nm^2 area. (4) H- and J-types of Sb(V)TSPP dimer formation occur in the excess area of the hybrid compound (Figure 8c).

The polyfluorinated microcavity, that is prepared by the intercalation of the polyfluorinated surfactants into the clay layer, has been shown to provide a very unique microenvironment that minimizes the solute−surrounding environment interaction and to relatively strengthen the intermolecular interaction between the solute molecules trapped in the microcavity. The polyfluorinated microcavity is a promisingly interesting microenvironment for examining various chemical reactions that could be governed by solute−solute interactions.

Acknowledgment. This work was partly supported by a Japan−US binational group research program (JSPS and NSF).

References and Notes

(1) Grim, R. E. *Clay Mineralogy*; McGraw-Hill: New York, 1953.

(2) Theng, B. K. *The Chemistry of Clay-Organic Reactions*; Adam Hilger: London, 1974.

(3) Van Olphen, H. *An Introduction to Clay Colloid Chemistry*, 2nd ed.; Wiley-Interscience: New York, 1977.

(4) Shiramizu, H. *Clay Mineralogy*; Asakura-shoten: Tokyo, 1988.

(5) Sposito, G.; Prost, R. *Chem. Rev.* **1982**, *82*, 553.

(6) *Intercalation Chemistry*; Whittingham, M. S., Jacobson, A. J., Eds.; Academic Press: New York, 1982.

(7) Ogawa, M.; Kuroda, K. *Chem. Rev.* **1995**, *95*, 399.

(8) Takagi, K.; Shichi, T. In *Solid State and Surface Photochemistry*; Ramamurthy, V., Schanze, K. S., Eds.; Marcel Dekker: New York, 2000; Vol. 5, p 31.

(9) Shichi, T.; Takagi, K. *J. Photochem. Photobiol., C* **2000**, *1*, 113.

(10) (a) Lagaly, G. *Clay Miner.* **1981**, *16*, 1. (b) Lagaly, G. *Clays Clay Miner.* **1982**, *30*, 215.

(11) (a) Weiss, A. *Chem. Ber.* **1958**, *91*, 487. (b) Weiss, A. *Angew. Chem.* **1963**, *75*, 113. (c) Weiss, A. *Angew. Chem., Int. Ed. Engl.* **1963**, *2*, 134.

(12) Okahata, Y.; Shimazu, A. *Langmuir* **1989**, *5*, 954.

(13) (a) Vaia, R. A.; Ishii, H.; Giannelis, E. P. *Chem Mater.* **1993**, *5*, 1694. (b) Vaia, R. A.; Teukolsky, R. K.; Giannelis, E. P. *Chem. Mater.* **1994**, *6*, 1017.

(14) Xu, S.; Boyd, S. A. *Langmuir* **1995**, *11*, 2508.

(15) (a) Ogawa, M.; Aono, T.; Kuroda, K.; Kato, C. *Langmuir* **1993**, *9*, 1529. (b) Ogawa, M.; Wada, T.; Kuroda, K. *Langmuir* **1995**, *11*, 4598.

(16) Yan, Y.; Bein, T. *Chem Mater.* **1993**, *5*, 905.

(17) Slade, P. G.; Raupach, M.; Emerson, W. W. *Clays Clay Miner.* **1978**, *26*, 125.

(18) (a) Banks, R. E. *Organofluorine Chemicals and their Industrial Applications*; Ellis Horwood Ltd.: Chichester, U.K., 1979. (b) Negishi, A. *Chemistry of Fluorine*; Maruzen: Tokyo, 1988. (c) Kitazumi, T.; Ishihara, T.; Taguchi, T. *Chemistry of Fluorine*; Kodansha Scientific: Tokyo, 1993.

(19) (a) Briks, J. B.; Christophorou, L. G. *Photophysics of Aromatic Molecules*; Birks, J. B., Eds.; John Wiley & Sons Ltd.: New York, 1969; Chapter 4. (b) Lawson, C. W.; Hirayama, F.; Lipsky, S. *J. Chem. Phys.* **1969**, *51*, 1590.

(20) (a) Horvath, I. T.; Rabai, J. *Science* **1994**, *266*, 72. (b) Myers, K. E.; Kumer, K. *J. Am. Chem. Soc.* **2000**, *122*, 12025.

(21) Kusaka, H.; Uno, M.; Kowald, M. K.; Ohmachi, T.; Kidokoro, S.; Yui, T.; Takagi, S.; Inoue, H. *Phys. Chem. Chem. Phys.* **1999**, *1*, 3135.

(22) Kameo, Y.; Takahashi, S.; Kowald, M. K.; Ohmachi, T.; Takagi, S.; Inoue, H. *J. Phys. Chem. B* **1999**, *103*, 9562.

(23) Yui, T.; Yoshida, H.; Tachibana, H.; Tryk, D. A.; Inoue, H. *Langmuir* **2002**, *18*, 891.

(24) Yui, T.; Uppili, S. R.; Shimada, T.; Tryk, D. A.; Yoshida, H.; Inoue, H. *Langmuir* **2002**, *18*, 4232.

(25) Matsuoka, R.; Yui, T.; Sasai, R.; Takagi, K.; Inoue, H. *Mol. Cryst. Liq. Cryst.* **2000**, *341*, 333.

(26) *The Porphyrin Handbook*; Kadish, K. M., Smith, K. M., Guilard, R., Eds.; Academic Press: New York, 1999.

(27) Takagi, S.; Inoue, H. In *Multimetallic and Macromolecular Inorganic Photochemistry*; Ramamurthy, V., Schanze, K. S., Eds.; Marcel Dekker: New York, 2000; Vol. 6, p 215.

(28) Shiragami, T.; Kubomura, K.; Ishibashi, D.; Inoue, H. *J. Am. Chem. Soc.* **1996**, *118*, 6311.

(29) (a) Takagi, S.; Suzuki, M.; Shiragami, T.; Inoue, H. *J. Am. Chem. Soc.* **1997**, *119*, 8712. (b) Takagi, S.; Morimoto, H.; Shiragami, T.; Inoue, H. *Res. Chem. Intermed.* **2000**, *23*, 171.

(30) Yamashita, K.; Kihara, N.; Shimidzu, H.; Suzuki, H. *Photochem. Photobiol.* **1982**, *35*, 1.

(31) Jones, R.; Tredgold, R. H.; Hoorfar, A. *Thin Solid Films* **1985**, *123*, 307.

(32) Beswick, R. B.; Pitt, C. W. *Chem. Phys. Lett.* **1988**, *143*, 589.

(33) Schick, G. A.; Schreiman, I. C.; Wagner, R. W.; Lindsey, J. S.; Bocian, D. F. *J. Am. Chem. Soc.* **1989**, *111*, 1344.

(34) Khairutdinov, R. F.; Serpone, N. *J. Phys. Chem. B* **1999**, *103*, 761.

(35) Maiti, N. C.; Mazumdar, S.; Periasamy, N. *J. Phys. Chem. B* **1998**, *102*, 1528.

(36) Hinoue, T.; Kobayashi, J.; Ozeki, T.; Watarai, H. *Chem. Lett.* **1997**, 763.

(37) (a) Osuka, A.; Maruyama, K. *J. Am. Chem. Soc.* **1988**, *110*, 4454. (b) Nagata, T.; Osuka, A.; Maruyama, K. *J. Am. Chem. Soc.* **1988**, *112*, 3054.

(38) (a) Usami, H.; Takagi, K.; Sawaki, Y. *J. Chem. Soc., Perkin. Trans. 2.* **1990**, 1723. (b) Takagi, S.; Shimada, T.; Yui, T.; Inoue, H. *Chem. Lett.* **2001**, 128. (c) Takagi, S.; Shimada, T.; Eguchi, M.; Yui, T.; Yoshida, H.; Tryk, D. A.; Inoue, H. *Langmuir* **2002**, *18*, 2265. (d) Takagi, S.; Tryk, D. A.; Inoue, H. *J. Phys. Chem. B* **2002**, *106*, 5455.

(39) Bilski, P.; Dabestani, R.; Chignell, C. F. *J. Phys. Chem.* **1991**, *95*, 5784.

(40) Yamaguchi, Y.; Yui, T.; Takagi, S.; Shimada, T.; Inoue, H. *Chem. Lett.* **2001**, 644.

(41) Relationship between solvent polarity and Soret absorption maxima of Sb(V)TSPP is as follows: H_2O (ϵ: 78.4; 415.0 nm), H_2O/methanol = 2:1 vol/vol (ϵ: 62.9; 416.4 nm), H_2O/methanol = 1:1 vol/vol (ϵ: 55.0; 417.5 nm), H_2O/methanol = 1:2 vol/vol (ϵ: 47.2; 418.0 nm), methanol (ϵ: 32.7; 418.6 nm), ethanol (ϵ: 24.6; 420.2 nm), cyclohexanone (ϵ: 18.3; 421.2 nm), pyridine (ϵ: 12.0; 429 nm).

(42) Kasah, M. *Radiat. Res.* **1963**, *20*, 50.

(43) (a) Shelnutt, A.; Dobry, M. M.; Satterlee, D. J. *J. Phys. Chem.* **1984**, *88*, 4980. (b) Shelnutt, J. A. *J. Phys. Chem.* **1984**, *88*, 4988.

(44) Calculated from the values of the surface area of the Sumecton SA (750 $m^2\ g^{-1}$) and CEC (0.998 meqv g^{-1}/g): 750 $m^2\ g^{-1}$/(0.998 meqv $g^{-1}\ N_A$) = 1.25 $nm^2\ eqv^{-1}$, where N_A is Avogadro's number.

(45) Li, B.; Fujii, M.; Fukuda, K.; Kato, T.; Seimiya, T. *J. Colloid Interface Soc.* **1999**, *209*, 25.

(46) Fujii, M.; Li, B.; Fukuda, K.; Kato, T.; Seimiya, T. *Langmuir* **2001**, *17*, 1138.

(47) Tsao, Y.-H.; Yang, S. X.; Evans, D. F. *Langmuir* **1991**, *10*, 3154.

(48) Sasai, R.; Shin'ya, N.; Shichi, T.; Takagi, K.; Gekko, K. *Langmuir* **1999**, *15*, 413.

(49) Sonobe, K.; Kikuta, K.; Takagi, K. *Chem. Mater.* **1999**, *11*, 1089.

(50) Sasai, R.; Shichi, T.; Gekko, K.; Takagi, K. *Bull. Chem. Soc. Jpn.* **2000**, *73*, 1925.

(51) Sasai, R.; Itoh, H.; Shindachi, I.; Shichi, T.; Takagi, K. *Chem. Mater.* **2001**, *13*, 2012.

(52) Michl, J.; Thulstrup, E. W. *Spectroscopy with Polarized Light*; VHC: New York, 1986; p 75.

(53) Fukuda, K.; Kato, T.; Nakahara, H.; Shibasaki, Y. *Chohaku-makubunsi Soshikimaku-no Kagaku*; Koudansha: Tokyo, 1993; p 89.